Premigratory and migratory neural crest cells are multipotent in vivo

Baggiolini, Arianna ; Varum, Sandra ; Mateos, José María ; Bettosini, Damiano ; John, Nessy ; Bonalli, Mario ; Ziegler, Urs ; Dimou, Leda ; Clevers, Hans ; Furrer, Reinhard ; Sommer, Lukas

Abstract: The neural crest (NC) is an embryonic stem/progenitor cell population that generates a diverse array of cell lineages, including peripheral neurons, myelinating Schwann cells, and melanocytes, among others. However, there is a long-standing controversy as to whether this broad developmental perspective reflects in vivo multipotency of individual NC cells or whether the NC is comprised of a heterogeneous mixture of lineage-restricted progenitors. Here, we resolve this controversy by performing in vivo fate mapping of single trunk NC cells both at premigratory and migratory stages using the R26R-Confetti mouse model. By combining quantitative clonal analyses with definitive markers of differentiation, we demonstrate that the vast majority of individual NC cells are multipotent, with only few clones contributing to single derivatives. Intriguingly, multipotency is maintained in migratory NC cells. Thus, our findings provide definitive evidence for the in vivo multipotency of both premigratory and migrating NC cells in the mouse.

DOI: https://doi.org/10.1016/j.stem.2015.02.017

Premigratory and Migratory Neural Crest Cells are Multipotent In Vivo

Arianna Baggiolini[1], Sandra Varum[1], José María Mateos[2], Damiano Bettosini[1], Nessy John[1], Mario Bonalli[1], Urs Ziegler[2], Leda Dimou[3], Hans Clevers[4], Reinhard Furrer[5], Lukas Sommer[1].

[1]Institute of Anatomy, University of Zurich, 8057 Zurich, Switzerland

[2]Center for Microscopy and Image Analysis, University of Zurich, 8057 Zurich, Switzerland

[3]Department of Physiological Genomics, Ludwig Maximilian University of Munich, 80336 Munich, Germany

[4]Hubrecht Institute, KNAW and University Medical Center Utrecht, Uppsalalaan 8, 3584 CT Utrecht, The Netherlands

[5]Institute of Mathematics, University of Zurich, 8057 Zurich, Switzerland

Correspondence: lukas.sommer@anatom.uzh.ch (L.S.)

SUMMARY

The neural crest (NC) is an embryonic stem/progenitor cell population that generates a diverse array of cell lineages, including peripheral neurons, myelinating Schwann cells, and melanocytes, among others. However, there is a long-standing controversy as to whether this broad developmental perspective reflects *in vivo* multipotency of individual NC cells, or whether the NC is comprised of a heterogeneous mixture of lineage-restricted progenitors. Here, we resolve this controversy by performing *in vivo* fate mapping of single trunk NC cells both at premigratory and migratory stages using the *R26R-Confetti* mouse model. By combining quantitative clonal analyses with definitive markers of differentiation, we demonstrate that the vast majority of individual NC cells are multipotent, with only few clones contributing to single derivatives. Intriguingly, multipotency is maintained in migratory NC cells. Thus, our findings provide definitive evidence for the *in vivo* multipotency of both premigratory and migrating NC cells in the mouse.

INTRODUCTION

Neural crest (NC) cells are a defining feature of vertebrates that give rise to many of the cell types that imbue them with their unique characteristics, such as jaws and peripheral nervous system. In the embryo, NC cells arise from the dorsal margin of the neural plate border during neurulation (Le Douarin et al., 2008), undergo an epithelial to mesenchymal transition (EMT), and migrate extensively throughout the embryo to populate numerous derivatives.

This has raised the important question of what underlies this remarkable ability to contribute to so many diverse derivatives, ranging from craniofacial cartilage to neurons and glia to melanocytes. One model suggests that the entire NC cell population is “multipotent” and capable of forming many or all of the potential derivatives. At the opposite extreme, the NC might instead represent a heterogeneous mixture of “predetermined” cells, each fated to form a particular derivative. Finally, the NC may be comprised of a mixture of these two types of precursor cells.

Over several decades, there has been considerable controversy regarding the correct answer to this pivotal question (Dupin and Sommer 2012). Early studies concluded that NC cells were multipotent *in vivo* (Bronner-Fraser and Fraser, 1988; Bronner-Fraser and Fraser, 1989; McKinney et al., 2013; Serbedzija et al., 1990) and *in vitro* (Baroffio et al., 1988; Dupin et al., 2010; Stemple and Anderson, 1992). However, other publications instead reported that the NC was comprised of heterogeneous populations of restricted progenitor cells (Harris and Erickson, 2007; Henion and Weston, 1997; Krispin et al., 2010). In particular, recent studies proposed that premigratory NC cells are fate-determined prior to delamination and organized according to a spatio-temporal pattern in the dorsal neural tube (dNT) of chick embryos (Krispin et al., 2010; Nitzan et al., 2013). In this model, each NC cell gives

rise only to a specific cell type, depending on the timing of emigration and the site of origin in the dNT.

Despite technical differences potentially explaining these discrepancies, it has so far not been possible to reconcile these studies (Dupin and Sommer, 2012). Early *in vivo* lineage tracing studies lacked the ability to identify specific cell types other than by location in various derivatives. Whereas clonal analysis *in vitro* circumvents these problems, the culture techniques analyze cells outside of their endogenous environment and expose cells to culture media, which may alter cell behavior. Moreover, there is very little information regarding the developmental potential of NC cells in mammalian model systems. Lineage-tracing studies were originally performed in chicken embryos by vital dye injection, which is very challenging to carry out in mouse embryos (Serbedzija et al., 1990). With the advent of modern transgenic technology, it is now possible to resolve the controversy regarding NC potentials in the mammalian embryo. Here, we use the *R26R-Confetti* mouse model to perform genetic *in vivo* fate mapping of NC cells. Our results definitively show that the vast majority of murine NC cells, both prior to and during migration, are multipotent.

RESULTS

Multicolor labeling of premigratory and migratory NC cells

To achieve temporal tracing of NC cells we used the *CreER loxP* system, by which activation of CreER recombinase can be induced in embryos in a cell type- and stage-dependent manner upon tamoxifen (TM) injection of pregnant females. CreER-mediated genomic recombination of reporter alleles leads to marker expression that can be tracked in CreER-expressing cells and all of their daughter cells, allowing fate mapping of these cells *in vivo*. To trace the fate of premigratory NC cells, we made use of *Wnt1-CreER^T* animals. Accordingly, *CreER^T*-induced β-

galactosidase expression in *Wnt1-CreER^{T}* embryos carrying the *CreER^{T}*-reporter allele *R26R-Rosa* was observed in the dNT and in all NC derivatives (Figures 1A and 1B) (Soriano, 1999; Zervas et al., 2004). To trace NC cells that have already emigrated from the dNT, we used the *Sox10-CreER^{T2}* line (Simon et al., 2012). In the mouse, Sox10 expression follows Wnt1 expression and marks virtually all NC cells immediately after their delamination from the dNT (Hari et al., 2012). Therefore, TM-induced recombination at E.9.0 in *Sox10-CreER^{T2} R26R-Rosa* embryos resulted in β-galactosidase expression in all NC derivatives, but not the dNT (Figures 1C and 1D).

Upon *CreER* activation and recombination across sets of loxP sites in the *R26R-Confetti* reporter mouse, one out of four fluorescent reporter proteins, nuclear GFP, cytoplasmic YFP, cytoplasmic RFP, or membrane-bound CFP, is expressed. To increase the colors available for the tracing, we used animals homozygous for the *R26R-Confetti* allele. In these animals, both alleles are recombined, which leads to expression of two out of the four available fluorescent proteins, allowing a total of 10 color combinations (Figure S1). In both *Wnt1-CreER^{T} R26R-Confetti* (hereafter called *Wnt1-CreER^{T}*) (Figures 1E-J) and in *Sox10-CreER^{T2} R26R-Confetti* (*Sox10-CreER^{T2}*) embryos (data not shown), expression of the following single color combinations was readily detectable: red (rfp, Figure 1E); yellow (yfp, Figure 1F); and blue (cfp, Figure 1G). In addition, we observed the expression of mixed color combinations, such as red and blue (rfp cfp, Figure 1H); red and yellow (rfp yfp, Figure 1I); yellow and blue (yfp cfp, Figure 1J). In contrast, color combinations with the fluorescent protein GFP were extremely rare, indicating that not all theoretically possible color combinations were equally represented.

Multicolor output depends on promoter activity and recombination density

The frequency of color combinations observed upon *CreER*-mediated recombination of a multicolor *Cre* reporter influences the probability of whether a cohort of cells

marked by a single color derives from one or more founder cells. Therefore, we examined the frequency of different colors expressed in E10.5 *R26R-Confetti* embryos of both *CreER* lines (Figure 1K). A single limiting dose of TM resulted in few recombination events. Quantification of low TM dose-treated E10.5 *Wnt1-CreER^{T} R26R-Confetti* embryos (*Wnt1-CreER$^{T\ low}$*) revealed that the mixed color combinations were expressed in only 0.1-0.9% of the recombined NC cells (Figure 1L and Table S1A). Similarly, in low TM dose-treated *Sox10-CreER^{T2} R26R-Confetti* embryos (*Sox10-CreER$^{T2\ low}$*) mixed colors were found at very low frequencies (Figure 1M and Table S1A). In contrast, the pure colors red, yellow, or blue were consistently expressed in recombined NC cells in both CreER lines (Figure 1L, 1M and Table S1A).

These findings prompted us to increase the level of recombination for both *CreER* lines, in order to obtain more NC cells expressing rare color combinations. For the *Wnt1-CreER^{T} R26R-Confetti* line, higher recombination density achieved by elevating the TM dose (*Wnt1-CreER$^{T\ high}$*) resulted in increased, but still low occurrence of the rare color combinations (0.3-3.2% of all recombined cells; Figure 1L, Table S1A). Similarly, elevating the TM concentration in the *Sox10-CreER^{T2} R26R-Confetti* line (*Sox10-CreER$^{T2\ high}$*) allowed increased representation of the mixed color combinations (1.0-3.5%; Figure 1M and Table S1A). Summarizing, in our system we were able to trace NC cells not only at two different developmental stages, namely at the premigratory and at the migratory stage, but also at two different recombination densities producing different color outputs. The most frequent color combinations allowed clonal tracing when only few recombination events occurred. Rare fluorescent marker combinations, on the other hand, could be used to discern single clones at both low and high recombination densities.

Representation frequencies of recombined NC cells in trunk derivatives

NC cells in the trunk of mouse embryos give rise to several structures, such as dorsal root ganglia (DRG), Schwann cells associated with peripheral nerves as, for instance, evident in the ventral root (VR), sympathetic ganglia (SG), and finally cells that migrate along the dorsal lateral pathway (DLP) to generate melanocytes. As expected, all these derivatives were marked in *Wnt1-CreER^{T}* and *Sox10-CreER^{T2}* embryos (Figures 2 A-F and data not shown). Moreover, tracing NC cells at the premigratory stage with the *Wnt1-CreER^{T}* line allowed the observation of recombined cells in the dNT, which we defined as the most dorsal three cell layers of the neural tube (Figures 2A and 2B).

The likelihood to detect daughter cells of a NC progenitor cell in different target structures is possibly dependent on the relative sizes of these structures: The bigger a given compartment, the more likely it might be for a daughter cell to end up in this compartment. In *Wnt1-CreER^{T}* embryos, we observed 7.6-14.0% of recombined cells in the dNT (Figure 2G and Table S1B), while no recombined cells were found in the dNT of *Sox10-CreER^{T2}* embryos. In all conditions, the majority of recombined cells were found in the biggest trunk NC derivative, the DRG (Figures 2C and 2G; Table S1B). The SG and the VR were populated by comparable numbers of recombined NC cells, while the DLP was the derivative with the lowest number of recombined cells (Figures 2D-G; Table S1B). Given the number of possible cell divisions in a time window of 41 hours (Figure 1K) the elevated numbers of some recombined cells of the same color in certain derivatives cannot be explained only by differential proliferation in these derivatives. Therefore, the fact that the majority of recombined cells were present in the bigger derivatives is likely due to higher numbers of migratory NC cells populating these derivatives.

Qualitative assessment of multicolor fate mapping of single premigratory NC cells

Our data reveal that *CreER*-mediated recombination of the *R26R-Confetti* allele allows tracking of NC cells by different color combinations at defined frequencies. We next exploited this system to track the fate of individual NC cells, with a first emphasis on premigratory cells. E10.5 embryos were collected 41 hours post TM injection (Figure 1K). As previously demonstrated, the mean cell cycle length of E9.5 NC cells is 10.6 hours (Gonsalvez et al., 2013). The literature does not provide exact error intervals for the cell division rate, and it is likely that during 41 hours of NC development the cell cycle length varies and becomes cell type- and derivative-specific. Since these variations are unknown and can hardly be determined, we first applied a fixed assumption that NC cells could divide 3 times between TM-induced recombination and the time point of analysis. Hence, we initially considered only equally colored cohorts of cells with a minimum of two and a maximum of eight cells, with the goal that such a stringent analysis would serve as a basis to establish and assess a statistical method able to discern between multipotency and cell fate restriction.

For the analysis of putative clones, we focused on the forelimbs area, taking into account cells of the same color that were present in a unit defined by a trunk segment spanning the width of one DRG (10-14 transverse sections of 10μm thickness each) (Figure S2 and Movie S1). 3D reconstruction confirmed that our recombination protocol allowed marking of a small number of equally colored NC daughter cells disseminating over various trunk derivatives (Figure S2 and Movie S1 and S2). Consecutive transverse sections at the level of the forelimbs were imaged (Figure S2Ai-xii), and the number and location of equally colored recombined cells per trunk segment were assessed (Figure 3). For the different conditions used, the

density of putative clones ranged between 0.8±0.1 and 1.0±0.3 clones per unit, with most units analyzed containing 0 or 1 clone (Table S2A). *Wnt1-CreER$^{T\ low}$* embryos displayed many putative clones with progeny in multiple derivatives, including sometimes the dNT and DLP (Figures 3A and S3A). To corroborate these results, we analyzed *Wnt1-CreER$^{T\ high}$* embryos, in which we observed cohorts of cells (2-8 cells) expressing rare mixed color combinations (Figures 3A and S3C). Strikingly, putative clones were mostly spread over multiple derivatives (Figures 3A and S3C).

Multicolor fate mapping of single migratory NC cells

Our findings prompted us to ask whether multipotency might be a unique characteristic of premigratory NC cells or whether this developmental potential is retained upon NC delamination and migration. Therefore, we analyzed the fate of NC cells in *Sox10-CreER^{T2}* embryos (Figure 1K). The clonal density found in *Sox10-CreER^{T2}* embryos was again low (Table S2A). Surprisingly, in *Sox10-CreER$^{T2\ low}$* embryos, many equally colored cell cohorts were dispersed over multiple NC derivatives, in a similar manner to what had been observed in *Wnt1-CreER^{T}* embryos (Figures 3B and S3B). Similar results were acquired for the *Sox10-CreER$^{T2\ high}$* embryos suggesting that these observations are independent of the recombination density and the color of the cell cohort (Figure 3B and S3D).

Statistical evaluation of cell fates adopted by premigratory and migratory NC cells

Our observations suggested that the majority of NC cells are multipotent both at the premigratory stage and, intriguingly, also at the migratory stage. To verify our results, we analyzed each data set considering the color of the observed putative clone, the derivative where we observed it, and its size. Defining the exact cell cycle length and its variation during a period of 41 hours for each specific derivative would have been extremely difficult and prone to mistakes. Thus, we applied a static framework

instead of a complete dynamic modeling approach. To distinguish between a predetermined and a multipotent framework for both *Wnt1-CreER^{T}* and *Sox10-CreER^{T2}* embryos, at low and high recombination levels, we calculated the respective probabilities of observing the specific clone configuration. Because the statistical model is based on count data, these probabilities are equivalent to likelihoods and thus twice the negative log of the likelihood ratio (deviance) was used to discriminate between the two frameworks (see Supplemental Experimental Procedures). To simplify the interpretation, the numerical values of the deviance were discretized into no, weak, substantial, and strong evidence for a framework of multipotency (Figure 3).

Based on this statistical evaluation, we first analyzed the cell cohorts (composed of 2-8 cells from the same color) obtained with the *Wnt1-CreER^{T}* embryos, pooling the data for low and high recombination densities. Strikingly, 65.1% (28 cases out of 43) of all uni-colored cell cohorts represented clones of the categories strong or substantial evidence for multipotency (Figures 3A and 3C). 27.9% (12 cases out of 43) of all cohorts analyzed were multipotent clones with more than 2 fates. In 18.6% (8 cases out of 43) of the clones, a progeny remained in the dNT. Half of these clones also contained cells in ventral structures as well as the DLP, demonstrating the broad developmental potential of the corresponding mother cells. Moreover, all uni-colored cell cohorts with derivatives in the DLP (18.6%, 8 cases out of 43) belonged to the category strong evidence for multipotency and contained NC-derived cells in at least one additional structure. Of all the cases analyzed, only 25.6% (11 cases out of 43) were belonging to the category no evidence for multipotency, indicating that lineage-restricted progenitor cells represent a minor fraction of premigratory NC cells (Figures 3A and 3C).

Unexpectedly, clones with strong or substantial evidence for multipotency were by far the most frequent categories also in the *Sox10-CreER*^{T2} embryos (70.2%, 33 cases out of 47) (Figures 3B and 3C). 31.9% (15 cases out of 47) of all cohorts analyzed were multipotent clones with progeny in only two derivatives (bi-fated) and 38.3% (18 cases out of 47) were clones with progeny in more than 2 derivatives; 24.2% (8 cases out of 33) of the uni-colored cell cohorts with substantial or strong evidence for multipotency contributed to the DLP (Figure 3B). Of note, all of these were multipotent clones with cells in the DLP and in at least one other structure, and half of the DLP-clones contained cells in as many as three additional NC derivatives. Similar to premigratory NC cells, fate-restricted migratory NC cells showing no evidence for multipotency were 21.3% (10 out of 47) of all clones (Figures 3B and 3C).

To assess the robustness of our statistical evaluation, we performed a sensitivity analysis by altering various parameters in the calculation of the multipotency likelihoods. When the minimum and maximum clone sizes were varied (rather than considering only clones of 2 to 8 cells), the resulting clone categories were still predominantly strong and substantial evidence for multipotency (Figure 3D). Furthermore, we perturbed the values of color frequency (r_{color}) and derivative size (d_{deriv}) (see Supplemental Experimental Procedures) by multiplying the probabilities and fractions by a random number between 1/3 and 3 (uniformly distributed), followed by rescaling. The analysis was carried out as described in the Supplemental Experimental Procedures, and the differences with respect to the evidence classification shown in Figure 3A and 3B were recorded. Figure 3E shows the results for 100 of such simulations and reveals that in both *Wnt1-CreER*^{T} and *Sox10-CreER*^{T2} *e*mbryos, the categorization of the clones into no, weak, substantial, and strong evidence for multipotency was not (low recombination densities) or only moderately changed (high recombination densities). Thus, even when challenged by modulating various parameters, our statistical evaluation consistently revealed that

the majority of premigratory and migratory NC cells were multipotent rather than fate restricted.

The statistical analysis presented in Figure 3 was performed under the stringent criteria that the maximum clone size was 8 cells. However, this clone size might not fully recapitulate the heterogeneity of embryonic cell populations, since it does not take into account the possibility that faster dividing cells might be present in distinct locations. Moreover, parameter modulation in our statistical analysis not only provided clear evidence for multipotency of NC cells, but also predicted that cell cohorts larger than the chosen range of 2-8 cells could also be actual clones. Therefore, we performed a further analysis, in which we considered all uni-colored cell cohorts found in defined trunk segments of *Wnt1-CreER^{T}* and *Sox10-CreER^{T2}* mice. To increase the probability of clonal tracing, we restricted this analysis to cell cohorts expressing rare colors only. The clonal density was low, ranging from 0.1±0.1 to 1.7±0.3 clones per unit (Table S2B). By applying the statistical analysis mentioned above we observed that the vast majority of the clones fell into the categories of strong or substantial evidence for multipotency, both in the *Wnt1-CreER^{T}* line (76.4%, 42 cases out of 55) and in the *Sox10-CreER^{T2}* line (75%, 36 cases out of 48) (Figure S4). Thus, including larger clones into our analysis did not affect the proportion of multipotent clones originating from premigratory and migratory NC cells, respectively, further demonstrating the robustness of our statistical analysis.

Multipotency assessed by differentiation marker analysis

During NC development, fate segregations are accompanied by spatial segregations of the resulting cell lineages. Therefore, a clone simultaneously located to multiple structures represents the progeny of a multipotent mother cell (Figures 3 and 4S). However, additional fate decisions are made within certain NC-derived structures, such as the DRG and SG, where neuronal lineages segregate from satellite glia. A

multipotent clone with cells in DRG and SG could thus be a neuron-only clone consisting of different types of neurons (sensory, autonomic), a glia-only clone with distinct types of glia (Wodhoo and Sommer, 2008), or a mixed neuron-glia clone. To address this issue, we performed an additional clonal analysis, taking into consideration not only the location of uni-colored NC cells, but also the expression of well-defined differentiation markers, such as Brn3a for sensory neurons, tyrosine hydroxylase (TH) for autonomic neurons, and Sox10 for glial and melanocytic cells. Groups of cells belonging to the rare color category were considered, without clonal size restriction (Figure 4). Only 4 out of 20 clones (*Wnt1-CreER^{T}* embryos) and 2 out of 16 clones (*Sox10-CreER^{T2}* embryos) were lineage restricted, respectively, meaning that these clones were not only confined to a single derivative, but they were also expressing only one marker of differentiation. Of note, of the 16 clones in *Wnt1-CreER^{T}* embryos that were not lineage-restricted, only 1 clone contained only neurons and no glia (clone ID 11; Figure 4A), while the other 14 clones were mixed neuron-glia clones. Likewise, 1 clone in *Sox10-CreER^{T2}* embryos contained sensory and sympathetic neurons but no glia (clone ID 11, Figure 4C), while all other multipotent clones were mixed neuronal and glial. Intriguingly, some of the cases that would have been considered to represent lineage-restricted clones based on their location, turned out to be at least bipotent, expressing multiple markers of differentiation (Figure 4A, clone IDs 13, 14, 15, 16; Figure 4C, clone IDs 13 and 14). These data substantiate our findings that single premigratory as well as single migratory NC cells mostly generate daughter cells that localize to distinct target structures and acquire different fates.

DISCUSSION

A fundamental question in developmental biology is how the distinct cell types of a given organ are established. Although it is thought that organ formation and homeostasis rely on the activity of organ-specific multipotent stem cells, several

recent publications demonstrated that heterogeneous populations of restricted progenitor cells, instead of multipotent mother cells, are often involved in the formation of vertebrate body structures (Lehoczky et al., 2011; Park et al., 2012). This issue is of particular interest with respect to the NC, because this structure represents one of the cell populations in the vertebrate embryo with the broadest developmental potential (Le Douarin et al., 2008). Several studies demonstrated that at least upon isolation, the majority of NC cells display stem cell features, being multipotent and able to self-renew (Dupin and Sommer, 2012). Others, however, reported the presence of many lineage-restricted cells in NC cell cultures (Harris and Erickson, 2007; Henion and Weston, 1997), suggesting that multipotency might be dependent on or even induced by culture conditions. The recent establishment of transgenic mouse lines allowing low density genetic recombination makes it possible to trace the lineage of single cells without the need of prior isolation and exposure of the cells to varying conditions. For instance, the *R26R-Confetti* reporter was used to track cells in the postnatal gut (Snippert et al., 2010). Here we applied this system to demonstrate that *in vivo* the NC cell population is primarily composed of multipotent cells rather than of a mixture of lineage-restricted precursors.

The *R26R-Confetti* mouse model offers the possibility to distinguish several clones from each other in the same specimen. Importantly, clonal analysis can be made in this system without prior cell isolation, transplantation, or any disturbance of the cellular microenvironment that might reactivate a “stemness” program (Snippert and Clevers, 2011). However, like in all retrospective lineage-tracing studies, redundant recombination events have to be excluded in the *R26R-Confetti* system to ensure clonal identification. To this end, we took advantage of the fact that theoretically equiprobable fluorescent protein combinations were expressed at different frequencies. In *Wnt1-CreER*^{T} mice, we were able to monitor the development of single premigratory NC cells at a low clonal density *in vivo* and to compare their fates

with those of migratory *Sox10-CreER^{T2}*-traced NC cells. Surprisingly, the range of fates and clonal distribution was very similar for these two settings. Most clones were distributed over several NC target structures and only in a minority of cases premigratory and migratory NC cells were fate restricted. Importantly, our statistical evaluation revealed a very high probability for multipotency, independent of color expression and recombination density. Moreover, subjecting our statistical evaluation to a sensitivity assay by altering multiple parameters, such as expected clone sizes and dimensions of the NC derivatives, confirmed the robustness of our method and the finding that most NC cells are multipotent.

Furthermore, the vast majority of clonal derivatives were not only spread over distinct locations, but also acquired distinct fates within given target structures. In particular, combining quantitative clonal assays with expression analysis of differentiation markers showed that the majority of NC cells, at least at the early stages analyzed, can neither be divided into “sensory-only” vs. “sympathetic-only”, nor into “neuron-only” vs. “glia-only” precursors.

In chicken embryos, DLP-colonizing NC cells are separate from ventrally migrating cells and belong to a late emigrating population (Erickson et al., 1992; Henion and Weston, 1997). We did not address here whether late emigrating NC cells exclusively destined to the DLP exist in mice. However, all clones with DLP contribution were multipotent in our study and contained cells in at least one ventral derivative. Thus, even after their emigration from the dNT, at least some mouse NC cells that will generate DLP derivatives maintain the potential to produce ventral neural cells.

Previous studies proposed that premigratory NC cells of the trunk are fate-restricted (Krispin et al., 2010; Nitzan et al., 2013). This result differed from earlier work that indicated the presence of multipotent premigratory NC cells, including “resident”

precursor cells for both CNS and NC in the dorsal neuroepithelium (Bronner-Fraser and Fraser, 1988; Bronner-Fraser and Fraser, 1989). These discrepancies might have been due to technical challenges and to differences in the stages and location of the labeled premigratory NC cells in the dNT. Although we cannot exclude differences in mechanisms of lineage segregation between avian and mammalian systems, our findings support the model, in which the majority of NC cells are multipotent not only at the population but also at the single cell level, and that multipotency is maintained in NC cells even after their emigration from the neural tube. However, we cannot rigorously exclude the existence of fate-restricted NC cells, as we found a minority of NC cells that appeared to give rise to only one derivative. It is therefore possible that the NC cell population contains a fraction of fate-restricted cells.

Even though most NC cells were multipotent in our study, the actual cell type composition varied in each clone, with some multipotent clones acquiring all possible fates and others producing only two cell types. This reflects the heterogeneous behavior of NC cells also seen in cell culture conditions permissive for multiple fates, where multipotency is frequently observed, but not fully realized by all cells (see e.g. Dupin et al., 2010; Stemple and Anderson, 1992). This heterogeneous behavior can be switched to a virtually homogeneous response when NC cells are exposed to instructive growth factors either *in vitro* (Shah et al., 1994) or *in vivo* (Hari et al, 2012). It remains to be shown whether, normally, fate choices by multipotent NC cells *in vivo* are purely stochastic.

Of note, we did not observe a pattern of restricted fate choices when we compared migratory with premigratory NC cells, speaking against gradual lineage restriction during NC development (Krispin et al. 2010; Le Douarin and Dupin, 1993), at least during the time window analyzed. Therefore, the multiple and variable fates adopted

by NC cells appear to reflect the dynamic behavior of stem cells in vertebrates as opposed to more deterministic lineage acquisitions observed in species such as *C. elegans* (Morrison et al., 1997).

Upon recombination at the premigratory stage, we found clones with recombined cells retained in the dNT, in addition to cells in NC derivatives. This may suggest an asymmetric division of NC cells and that a resident “stem cell” population is established in the dorsal midline. Moreover, multipotency was maintained in migratory NC cells. Together, these findings are consistent with the hypothesis that neural crest stem cells (NCSCs) as originally characterized in cell culture (Stemple and Anderson, 1992) might not only be *in vitro* stem cells (Smith, 2006), but actually exist *in vivo*. In support of this hypothesis, undifferentiated NC-derived cells in the sciatic nerve were shown before to be able to self-renew *in vivo* and to maintain their multipotency as revealed upon isolation (Morrison et al., 1999). However, to demonstrate self-renewal and maintenance of multipotency by single NC cells *in vivo* without cell isolation or disturbing the cellular microenvironment would be technically challenging due to the dissemination of NC cells within a short time period. Concluding, our study demonstrates that the majority of NC cells are multipotent, both at the premigratory and at the migratory stage.

EXPERIMENTAL PROCEDURES

Mice

Mice homozygous for the *R26R Confetti* allele (Snippert et al., 2010) were crossed with the two inducible mouse lines *Wnt1-CreER^{T}* (Zervas et al., 2004) and *Sox10-CreER^{T2}* (Simon et al., 2012). All the embryos used in the analyses were derived from a 2 hours time-mating. Lineage tracing of premigratory NC cells at low and high recombination densities was achieved with pregnant *Wnt1-CreER^{T} R26R-Confetti* homozygous females, injected at E9.0. The animals were injected i.p. with a single limiting dose of 7.5μg and 50μg tamoxifen/g body weight for low and high recombination densities, respectively. Similarly, to recombine migratory NC cells we injected i.p. pregnant *Sox10-CreER^{T2} R26R-Confetti* homozygous animals at E9.0 with a single dose of 50μg or 150μg tamoxifen/g body weight to induce low or high recombination densities, respectively. Finally, embryos were collected at E10.5, 41 hours post TM injection. Animal experiments were approved by the veterinary office of the Canton of Zurich, Switzerland.

Microscopy

Images were acquired using a Leica CTR600 microscope and a Confocal Laser Scanning Microscopy (Leica CLSM SP5). For the Rosa four-color imaging, scans were performed in a series for fluorescent protein excitation as described in (Snippert et al., 2011).

Data analysis

The data analysis was performed using R version 3.1.1. R Development Core Team (2014). R: A language and environment for statistical computing. Vienna, Austria. ISBN 3-900051-07-0, URL http://www.R-project.org.

SUPPLEMENTAL INFORMATION

Supplemental Information includes Supplemental Experimental Procedures, 4 figures, 2 movies and 2 tables.

ACKNOWLEDGMENTS

We thank Sherif Idriss and Justin Strauss for their contributions to the collection of the data. We thank Prof. Alexandra Joyner for sharing the *Wnt1-CreER*^{T} mouse line and Prof. Marianne Bronner for her critical reading of the manuscript. This study was supported by the Swiss National Science Foundation, the National Research Program (NRP-63) "Stem Cells and Regenerative Medicine", and the University Research Priority Programs (URPPs) “Translational Cancer Research” and “Systems Biology/Functional Genomics”.

References

Baroffio, A., Dupin, E., and Douarin, N.M.L. (1988). Clone-forming ability and differentiation potential of migratory neural crest cells. PNAS *85*, 5325–5329.

Bronner-Fraser, M., and Fraser, S. (1988). Cell lineage analysis reveals multipotency of some avian neural crest cells. Nature *335*, 161–164.

Bronner-Fraser, M., and Fraser, S. (1989). Developmental potential of avian trunk neural crest cells in situ. Neuron *3*, 755–766.

Dupin, E., and Sommer, L. (2012). Neural crest progenitors and stem cells: From early development to adulthood. Developmental Biology *366*, 83–95.

Dupin, E., Calloni, G.W., and Le Douarin, N.M. (2010). The cephalic neural crest of amniote vertebrates is composed of a large majority of precursors endowed with neural, melanocytic, chondrogenic and osteogenic potentialities. Cell Cycle *9*, 238–249.

Erickson, C.A., Duong, T.D., and Tosney, K.W. (1992). Descriptive and experimental analysis of the dispersion of neural crest cells along the dorsolateral path and their entry into ectoderm in the chick embryo. Developmental Biology *151*, 251–272.

Gonsalvez, D.G., Cane, K.N., Landman, K.A., Enomoto, H., Young, H.M., and Anderson, C.R. (2013). Proliferation and Cell Cycle Dynamics in the Developing Stellate Ganglion. J. Neurosci. *33*, 5969–5979.

Hari, L., Miescher, I., Shakhova, O., Suter, U., Chin, L., Taketo, M., Richardson, W.D., Kessaris, N., and Sommer, L. (2012). Temporal control of neural crest lineage generation by Wnt/β-catenin signaling. Development *139*, 2107–2117.

Harris, M.L., and Erickson, C.A. (2007). Lineage specification in neural crest cell

pathfinding. Dev. Dyn. Off. Publ. Am. Assoc. Anat. *236*, 1–19.

Henion, P.D., and Weston, J.A. (1997). Timing and pattern of cell fate restrictions in the neural crest lineage. Development *124*, 4351–4359.

Krispin, S., Nitzan, E., Kassem, Y., and Kalcheim, C. (2010). Evidence for a Dynamic Spatiotemporal Fate Map and Early Fate Restrictions of Premigratory Avian Neural Crest. Development *137*, 585–595.

Le Douarin, N.M., Calloni, G.W., and Dupin, E. (2008). The stem cells of the neural crest. Cell Cycle *7*, 1013–1019.

Lehoczky, J.A., Robert, B., and Tabin, C.J. (2011). Mouse digit tip regeneration is mediated by fate-restricted progenitor cells. Proc Natl Acad Sci U S A *108*, 20609–20614.

McKinney, M.C., Fukatsu, K., Morrison, J., McLennan, R., Bronner, M.E., and Kulesa, P.M. (2013). Evidence for dynamic rearrangements but lack of fate or position restrictions in premigratory avian trunk neural crest. Development *140*, 820–830.

Morrison, S.J., White, P.M., Zock, C., and Anderson, D.J. (1999). Prospective identification, isolation by flow cytometry, and in vivo self-renewal of multipotent mammalian neural crest stem cells. Cell *96*, 737–749.

Nitzan, E., Krispin, S., Pfaltzgraff, E.R., Klar, A., Labosky, P.A., and Kalcheim, C. (2013). A dynamic code of dorsal neural tube genes regulates the segregation between neurogenic and melanogenic neural crest cells. Development *140*, 2269–2279.

Park, D., Spencer, J.A., Koh, B.I., Kobayashi, T., Fujisaki, J., Clemens, T.L., Lin, C.P., Kronenberg, H.M., and Scadden, D.T. (2012). Endogenous Bone Marrow

MSCs Are Dynamic, Fate-Restricted Participants in Bone Maintenance and Regeneration. Cell Stem Cell *10*, 259–272.

Serbedzija, G.N., Fraser, S.E., and Bronner-Fraser, M. (1990). Pathways of Trunk Neural Crest Cell Migration in the Mouse Embryo as Revealed by Vital Dye Labelling. Development *108*, 605–612.

Shah, N.M., Marchionni, M.A., Isaacs, I., Stroobant, P., and Anderson, D.J. (1994). Glial growth factor restricts mammalian neural crest stem cells to a glial fate. Cell *77*, 349–360.

Simon, C., Lickert, H., Götz, M., and Dimou, L. (2012). Sox10-iCreERT2: A mouse line to inducibly trace the neural crest and oligodendrocyte lineage. Genesis *50*, 506–515.

Smith, A. (2006). A glossary for stem-cell biology. Nature *441*, 1060–1060.

Snippert, H.J., and Clevers, H. (2011). Tracking adult stem cells. EMBO Rep. *12*, 113–122.

Snippert, H.J., van der Flier, L.G., Sato, T., van Es, J.H., van den Born, M., Kroon-Veenboer, C., Barker, N., Klein, A.M., van Rheenen, J., Simons, B.D., et al. (2010). Intestinal Crypt Homeostasis Results from Neutral Competition between Symmetrically Dividing Lgr5 Stem Cells. Cell *143*, 134–144.

Soriano, P. (1999). Generalized lacZ expression with the ROSA26 Cre reporter strain. Nat. Genet. *21*, 70–71.

Stemple, D.L., and Anderson, D.J. (1992). Isolation of a stem cell for neurons and glia from the mammalian neural crest. Cell *71*, 973–985.

Woodhoo, A., and Sommer, L. (2008). Development of the Schwann cell lineage:

from the neural crest to the myelinated nerve. Glia *56*, 1481–1490.

Zervas, M., Millet, S., Ahn, S., and Joyner, A.L. (2004). Cell Behaviors and Genetic Lineages of the Mesencephalon and Rhombomere 1. Neuron *43*, 345–357.

Figure Legends

Figure 1. Multicolor tracing of premigratory and migratory NC cells

(A-B) β-Galactosidase expression in premigratory NC cells in E9.5 and E12.5 *Wnt1-CreER^{T} R26R* embryos, and in migratory NC cells in *Sox10-CreER^{T2} R26R* embryos (C-D). (E-J) *In vivo* expression of the single color combinations rfp (E), yfp (F), cfp (G) and of the mixed color combinations rfp cfp (H), rfp yfp (I), yfp cfp (J). Neurofilament staining (NF, in white) delineates the structure of the dorsal root ganglia (DRG). (K) Experimental outline for the multicolor lineage-tracing approach. E0, embryonic day 0; p.i., post injection of tamoxifen. (L-M) Frequencies of the color combinations in the four cases analyzed (*Wnt1-CreER^{T}* and *Sox10-CreER^{T2}* at low and high recombination densities). For numbers of analyzed embryos see Supplemental Experimental Procedures. Scale bars: 50 μm. See also Figure S1 and Table S1A.

Figure 2. Frequencies of genetically traced cells in trunk derivatives of the NC

(A) Schematic drawing of a transverse section with NC cells (in red) in the dorsal lateral pathway containing cells of the melanocytic lineage (DLP), sensory dorsal root ganglia (DRG), sympathetic ganglia (SG), and ventral root with Schwann cells (VR). Recombined NC cells are found *in vivo* in the dNT (B), DRG (C), VR (D), SG (E), and DLP (F). (G) Percentages of recombined cells per derivative in *Wnt1*-CreER^{T} and Sox10-CreER^{T2} embryos at low and high recombination densities, respectively. For numbers of analyzed embryos see Supplemental Experimental Procedures. Scale bars: 50 μm. See also Table S1B.

Figure 3. Lineage tracing analysis of premigratory and migratory NC cells and mathematical evaluation of fate determination in NC cells

List of the clonal frameworks for premigratory (A) and migratory (B) NC cells ordered by degree of evidence for multipotency. Both conditions of low and high recombination densities were pooled to compare exclusively premigratory versus migratory NC. (C) Percentages of clones expressing no, weak, substantial and strong evidence of multipotency for both premigratory and migratory NC cells at low and high recombination densities. (D) Degrees of evidence for multipotency when the minimum and the maximum size of a clone were changed for premigratory and migratory NC at low and high recombination densities. (E) Sensitivity assay of the statistical evaluation method. Each of the 16 barplots shows the proportion of cases that changed (ranging from loss of 4 clones up to gain of 4 clones) upon 100 different simulations. White indicates no change, red cases that were added and green cases that were lost. See also Figures S2, S3 and S4. For numbers of analyzed embryos see Supplemental Experimental Procedures.

Figure 4. Quantitative clonal assays combined with differentiation marker analysis

List of the clonal frameworks for premigratory (A) and migratory (C) NC cells ordered by degree of evidence for multipotency. Only clones belonging to the rare color category where analyzed, and no size restriction was applied. Each single clone was analyzed in regard to its location and expression of the following differentiation markers: Brn3a, a sensory neuron marker; tyrosine hydroxylase (TH), a sympathetic neuron marker; and Sox10 that at this developmental stage labels glial and melanocytic lineages. (B and D) Schemes summarizing the distribution of entire clones respectively found in *Wnt1-CreER*^{T} and *Sox10-CreER*^{T2} embryos at high recombination densities. (Bi-Biii and Di-Diii) Examples of embryonic sections through NC derivatives that comprise rare color-expressing cells belonging to the clones

shown in (B) and (D), respectively. For numbers of analyzed embryos see Supplemental Experimental Procedures. Scale bars: 50 μm.

Figure 1

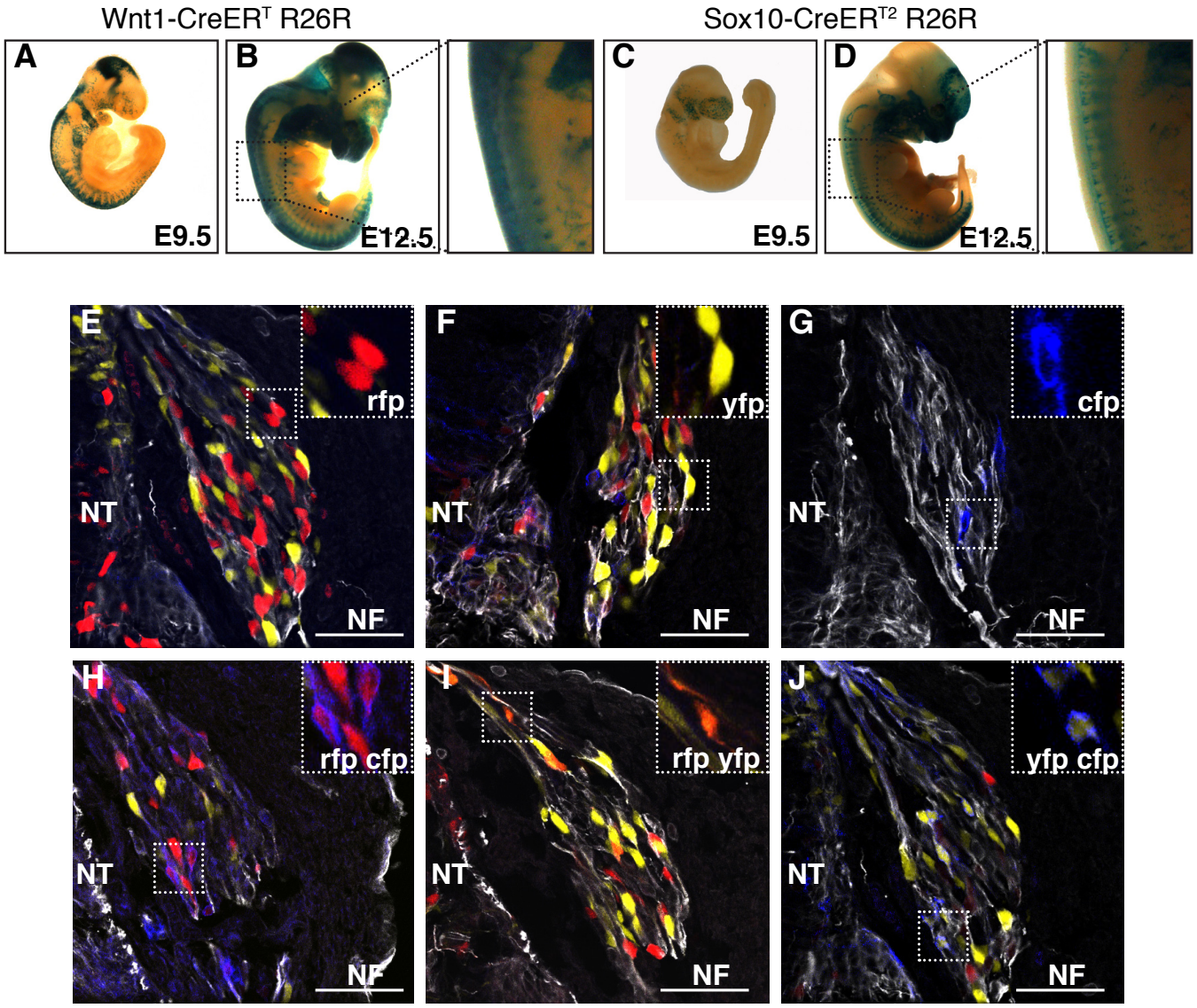
Wnt1-CreER^{T} R26R
Sox10-CreER^{T2} R26R
A
E9.5
B
E12.5
C
E9.5
D
E12.5
E
rfp
NT
NF
F
yfp
NT
NF
G
cfp
NT
NF
H
rfp cfp
NT
NF
I
rfp yfp
NT
NF
J
yfp cfp
NT
NF
K
Time mating
2h interval
E0
E9
Tamoxifen pulse
41h p.i.
Histological analysis
L
Frequency of color combinations (%)
Wnt1-CreER^{T} low
n = 7
Wnt1-CreER^{T} high
n = 18
rfp
yfp
cfp
rfp cfp
rfp yfp
yfp cfp
gfp
gfp yfp
gfp rfp
gfp cfp
M
Frequency of color combinations (%)
Sox10-CreER^{T2} low
n = 4
Sox10-CreER^{T2} high
n = 10
rfp
yfp
cfp
rfp cfp
rfp yfp
yfp cfp
gfp
gfp yfp
gfp rfp
gfp cfp

Figure 2

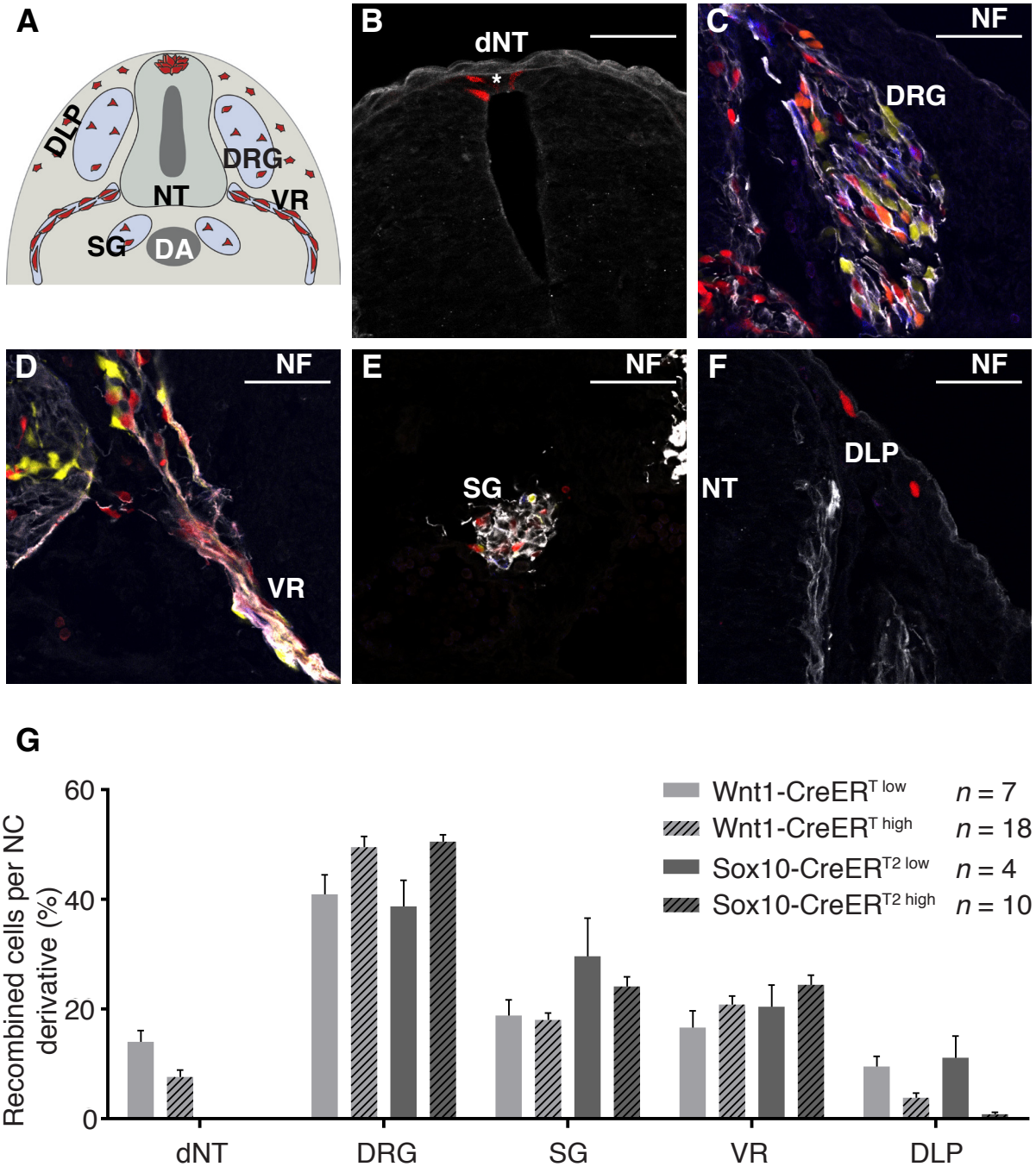
A
DLP
DRG
NT
VR
SG
DA
B
dNT
*
C
NF
DRG
D
NF
VR
E
NF
SG
F
NF
DLP
NT
G
Recombined cells per NC derivative (%)
60
40
20
0
dNT
DRG
SG
VR
DLP
Wnt1-CreER^T low n = 7
Wnt1-CreER^T high n = 18
Sox10-CreER^T2 low n = 4
Sox10-CreER^T2 high n = 10

Figure 3

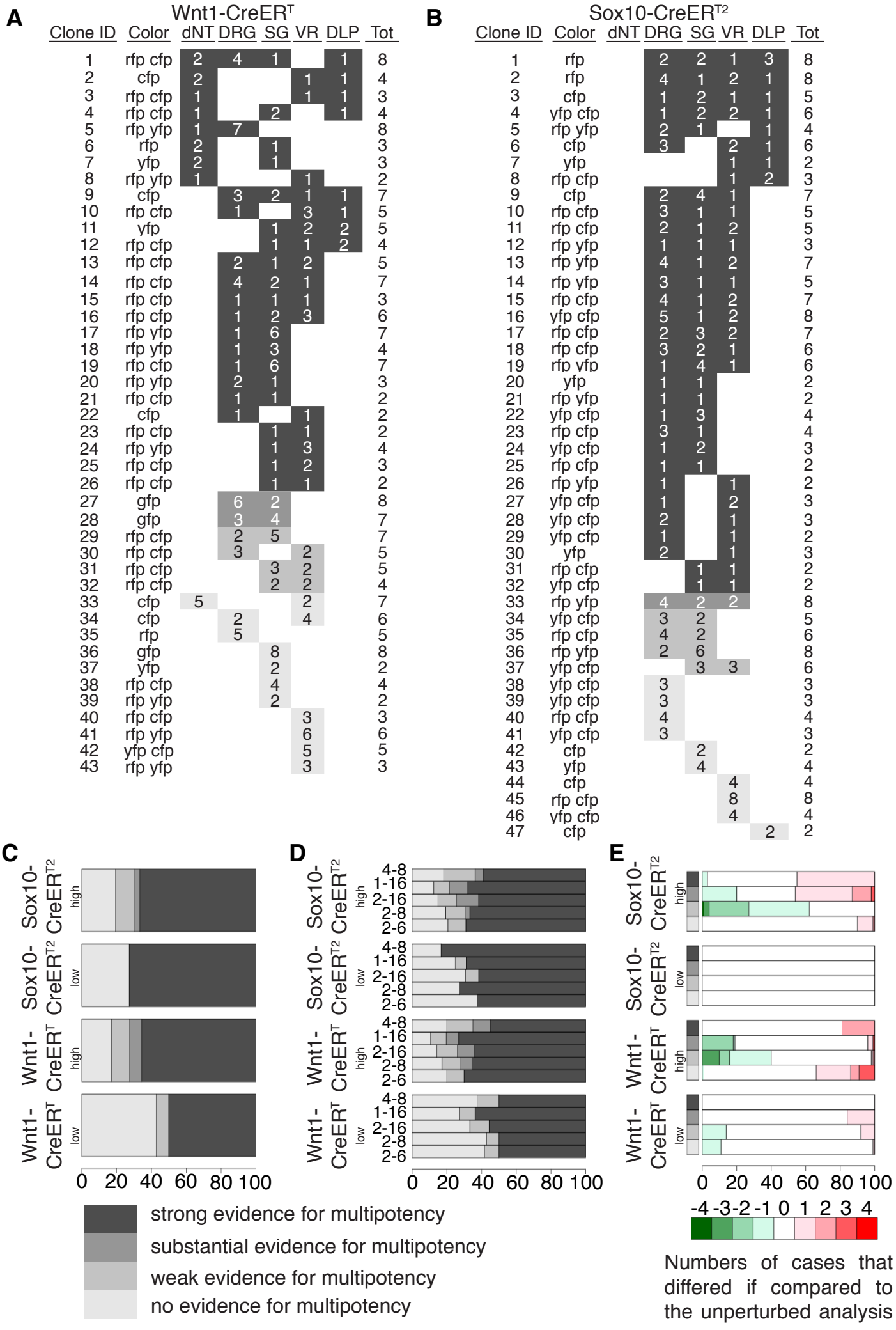
A
Wnt1-CreER^T
Clone ID Color dNT DRG SG VR DLP Tot
1 rfp cfp 2 4 1 1 8
2 cfp 2 1 1 4
3 rfp cfp 1 1 1 3
4 rfp cfp 1 2 1 4
5 rfp yfp 1 7 8
6 rfp 2 1 3
7 yfp 2 1 3
8 rfp yfp 1 1 2
9 cfp 3 2 1 1 7
10 rfp cfp 1 3 1 5
11 yfp 1 2 2 5
12 rfp cfp 1 1 2 4
13 rfp cfp 2 1 2 5
14 rfp cfp 4 2 1 7
15 rfp cfp 1 1 1 3
16 rfp cfp 1 2 3 6
17 rfp yfp 1 6 7
18 rfp yfp 1 3 4
19 rfp cfp 1 6 7
20 rfp yfp 2 1 3
21 rfp cfp 1 1 2
22 cfp 1 1 2
23 rfp cfp 1 1 2
24 rfp yfp 1 3 4
25 rfp cfp 1 2 3
26 rfp cfp 1 1 2
27 gfp 6 2 8
28 gfp 3 4 7
29 rfp cfp 2 5 7
30 rfp cfp 3 2 5
31 rfp cfp 3 2 5
32 rfp cfp 2 2 4
33 cfp 5 2 7
34 cfp 2 4 6
35 rfp 5 5
36 gfp 8 8
37 yfp 2 2
38 rfp cfp 4 4
39 rfp yfp 2 2
40 rfp cfp 3 3
41 rfp yfp 6 6
42 yfp cfp 5 5
43 rfp yfp 3 3
B
Sox10-CreER^T2
Clone ID Color dNT DRG SG VR DLP Tot
1 rfp 2 2 1 3 8
2 rfp 4 1 2 1 8
3 cfp 1 2 1 1 5
4 yfp cfp 1 2 2 1 6
5 rfp yfp 2 1 1 4
6 cfp 3 2 1 6
7 yfp 1 1 2
8 rfp cfp 1 2 3
9 cfp 2 4 1 7
10 rfp cfp 3 1 1 5
11 rfp cfp 2 1 2 5
12 rfp yfp 1 1 1 3
13 rfp yfp 4 1 2 7
14 rfp yfp 3 1 1 5
15 rfp cfp 4 1 2 7
16 yfp cfp 5 1 2 8
17 rfp cfp 2 3 2 7
18 rfp cfp 3 2 1 6
19 rfp yfp 1 4 1 6
20 yfp 1 1 2
21 rfp yfp 1 1 2
22 yfp cfp 1 3 4
23 rfp cfp 3 1 4
24 yfp cfp 1 2 3
25 rfp cfp 1 1 2
26 rfp yfp 1 1 2
27 yfp cfp 1 2 3
28 yfp cfp 2 1 3
29 yfp cfp 1 1 2
30 yfp 2 1 3
31 rfp cfp 1 1 2
32 yfp cfp 1 1 2
33 rfp yfp 4 2 2 8
34 yfp cfp 3 2 5
35 rfp cfp 4 2 6
36 rfp yfp 2 6 8
37 yfp cfp 3 3 6
38 yfp cfp 3 3
39 yfp cfp 3 3
40 rfp cfp 4 4
41 yfp cfp 3 3
42 cfp 2 2
43 yfp 4 4
44 cfp 4 4
45 rfp cfp 8 8
46 yfp cfp 4 4
47 cfp 2 2
C
Sox10-CreER^T2 high
Sox10-CreER^T2 low
Wnt1-CreER^T high
Wnt1-CreER^T low
0 20 40 60 80 100
D
4-8
1-16
2-16
2-8
2-6
0 20 40 60 80 100
E
-4 -3 -2 -1 0 1 2 3 4
strong evidence for multipotency
substantial evidence for multipotency
weak evidence for multipotency
no evidence for multipotency
Numbers of cases that differed if compared to the unperturbed analysis

Figure 4

A

Wnt1-CreER$^{T\ high}$

Clone ID	Color	dNT	DRG		SG		VR	DLP	Tot
			Sox10	Brn3a	Sox10	TH	Sox10	Sox10	
1	rfp yfp	2	3	7	2	1	4	2	21
2	rfp yfp	7	3	17	1	2	4		34
3	rfp yfp	1	5	4	3	1			14
4	rfp yfp	1	14	3		1	1		20
5	rfp yfp	3	3		1	2	4		13
6	rfp cfp	2					2		4
7	rfp yfp		4	2	1				7
8	rfp yfp		3			3		1	7
9	rfp cfp		2			2			4
10	rfp yfp			9	1	4			15
11	rfp yfp			6		1			7
12	rfp yfp			2			8		10
13	rfp yfp		1	1					2
14	rfp yfp		1	2					3
15	rfp yfp				1	2			3
16	rfp yfp				1	4			5
17	rfp cfp	4							4
18	rfp yfp			3					3
19	yfp cfp					2			2
20	yfp cfp					2			2

B

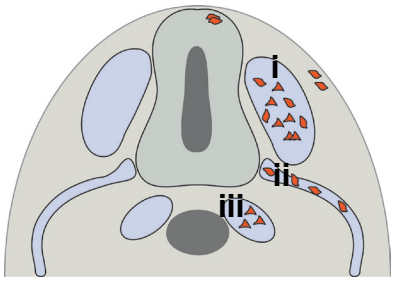

Wnt1-CreER$^{T\ high}$ clone number 1

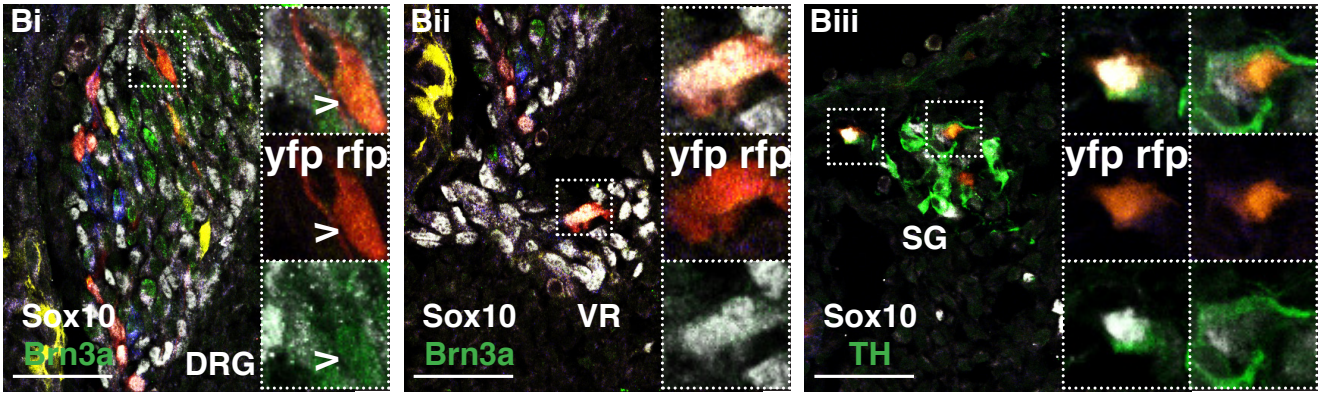

C

Sox10-CreER$^{T2\ high}$

Clone ID	Color	dNT	DRG		SG		VR	DLP	Tot
			Sox10	Brn3a	Sox10	TH	Sox10	Sox10	
1	rfp yfp		4	6	2	1	4		17
2	rfp yfp		7	5	1	1	1		15
3	rfp yfp		4	1	1	6	7		19
4	rfp cfp		3	2	1	1			7
5	rfp yfp		1	2	7				10
6	yfp cfp		1	1		1			3
7	rfp yfp		1	2		1			4
8	yfp cfp		1	1			1		3
9	yfp cfp		1	1			1		3
10	rfp cfp		2			2			4
11	rfp yfp			2		2			4
12	rfp cfp					1	1		2
13	yfp cfp		1	2					3
14	rfp yfp		2	10					12
15	rfp yfp		2						2
16	yfp cfp		2						2

D

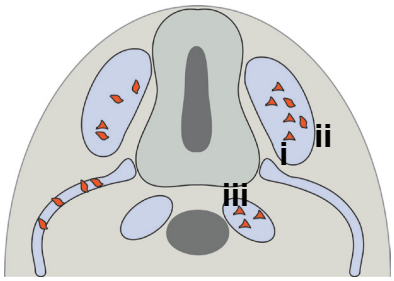

Sox10-CreER$^{T2\ high}$ clone number 1

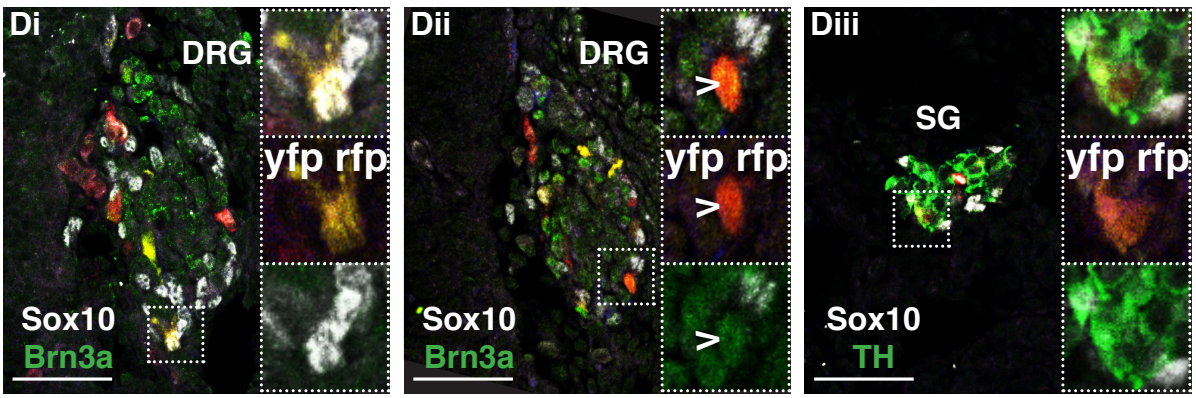

Supplemental Information

Premigratory and Migratory Neural Crest Cells are Multipotent In Vivo

Arianna Baggiolini[1], Sandra Varum[1], José María Mateos[2], Damiano Bettosini[1], Nessy John[1], Mario Bonalli[1], Urs Ziegler[2], Leda Dimou[3], Hans Clevers[4], Reinhard Furrer[5], Lukas Sommer[1].

[1]Institute of Anatomy, University of Zurich, 8057 Zurich, Switzerland

[2]Center for Microscopy and Image Analysis, University of Zurich, 8057 Zurich, Switzerland

[3]Department of Physiological Genomics, Ludwig Maximilian University of Munich, 80336 Munich, Germany

[4]Hubrecht Institute, KNAW and University Medical Center Utrecht, Uppsalalaan 8, 3584 CT Utrecht, The Netherlands

[5]Institute of Mathematics, University of Zurich, 8057 Zurich, Switzerland

Figure S1 related to Figure 1

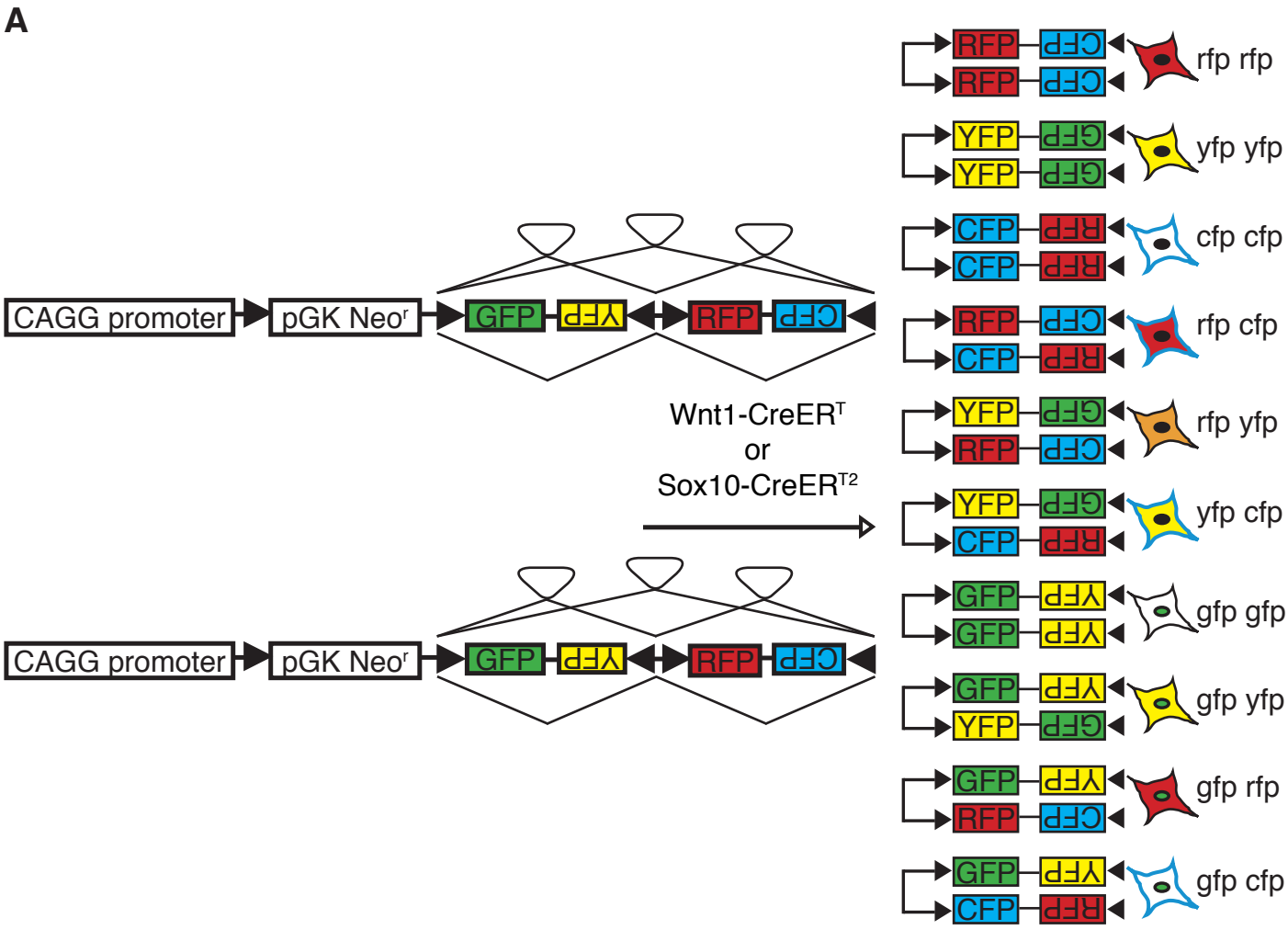

FIGURE S1: Related to Figure 1. The R262-Confetti construct.

(A) Confetti construct inserted in the *Rosa26* locus. Upon *Wnt1-CreER*^{T} or *Sox10-CreER*^{T2} activation, recombination occurs across different pairs of *loxP* sites and results in expression of one out of the four possible fluorescent reporter proteins: nuclear GFP, membrane-associated CFP, cytoplasmic RFP, cytoplasmic YFP. Recombination in embryos homozygous for the *R26R*-Confetti allele allows up to ten different fluorescent proteins combinations. For the single color combinations, rfp, yfp and cfp, the recombination of only one of the two *R26R-Confetti* alleles cannot be excluded, since limiting dosages of TM were used.

Figure S2 related to Figure 2

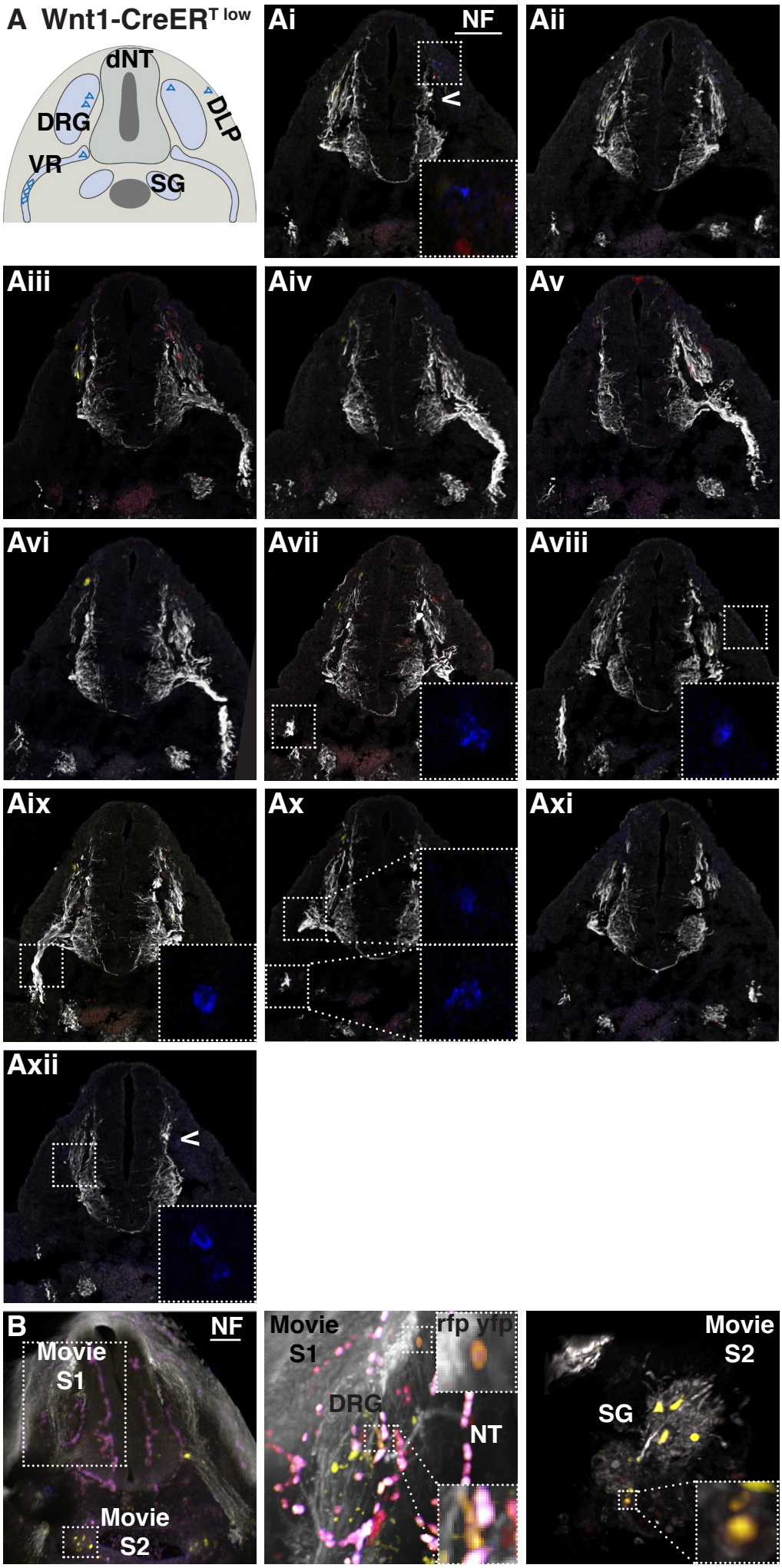

FIGURE S2: Related to Figure 2. DRG-unit and clone representations.

(A) Schematic summary of an 8-cells cfp^+ clone analyzed in an E10.4 *Wnt1*-$CreER^{T\ low}$ embryo. (Ai-Axii) Pictures of all transversal embryonic sections spanning the entire DRG-unit, in which the cfp^+ clone was observed. Arrows in Ai and Axii indicate the beginning and the end of the DRG-unit. (B) Z 316.7 μm stack of the trunk segment of an E10.5 *Wnt1-CreER*$^{T\ high}$ embryo, which has been used to produce Movie S1 and Movie S2. Scale bars: 100 μm.

Figure S3 related to Figure 3

strong evidence for multipotency

substantial evidence for multipotency

weak evidence for multipotency

no evidence for multipotency

A Wnt1-CreER$^{T\ low}$

Clone ID	Color	dNT	DRG	SG	VR	DLP	Tot
1	rfp cfp	1		2		1	4
2	rfp cfp	1			1	1	3
3	rfp	2		1		1	4
4	cfp		3	2	1	1	7
5	rfp yfp	1			1		2
6	rfp cfp		1	2	3		6
7	rfp yfp			1	3		4
8	yfp cfp			2	2		4
9	cfp	5			2		7
10	yfp			2			2
11	rfp cfp			4			4
12	rfp yfp			2			2
13	yfp cfp				5		5
14	rfp yfp				3		3

B Sox10-CreER$^{T2\ low}$

Clone ID	Color	dNT	DRG	SG	VR	DLP	Tot
1	rfp		2	2	1	3	8
2	rfp		4	1	2	1	8
3	cfp		1	2	1	1	5
4	yfp				1	1	2
5	rfp cfp		3	1	1		5
6	cfp		2	4	1		7
7	yfp		1	1			2
8	yfp		2		1		3
9	cfp			2			2
10	yfp			4			4
11	cfp				2		2

C Wnt1-CreER$^{T\ high}$

Clone ID	Color	dNT	DRG	SG	VR	DLP	Tot
1	rfp cfp	2	4	1		1	8
2	cfp	2			1	1	4
3	rfp yfp	1	7				8
4	yfp	2		1			3
5	rfp cfp		1		3	1	5
6	yfp			1	2	2	5
7	rfp cfp			1	1	2	4
8	rfp cfp		1	1	1		3
9	rfp cfp		4	2	1		7
10	rfp cfp		2	1	1		4
11	rfp yfp		1	3			4
12	rfp yfp		1	6			7
13	rfp cfp			1	1		2
14	rfp cfp		1	1			2
15	rfp cfp		1	6			7
16	rfp yfp		2	1			3
17	cfp		1		1		2
18	rfp cfp			1	1		2
19	rfp cfp			1	2		3
20	gfp		6	2			8
21	gfp		3	4			7
22	rfp cfp		2	5			7
23	rfp cfp		3		2		5
24	rfp cfp			3	2		5
25	cfp		2		4		6
26	rfp		5				5
27	gfp			8			8
28	rfp cfp				3		3
29	rfp yfp				6		6

D Sox10-CreER$^{T2\ high}$

Clone ID	Color	dNT	DRG	SG	VR	DLP	Tot
1	yfp cfp		1	2	2	1	6
2	rfp yfp		2	1		1	4
3	cfp		3		2	1	6
4	rfp cfp				1	2	3
5	rfp yfp		4	1	2		7
6	rfp yfp		1	4	1		6
7	rfp cfp		4	1	2		7
8	yfp cfp		5	1	2		8
9	rfp cfp		2	3	2		7
10	rfp yfp		3	1	1		5
11	rfp cfp		3	2	1		6
12	rfp yfp		1	1	1		3
13	rfp cfp		2	1	2		5
14	yfp cfp		1	2			3
15	rfp yfp		1	1			2
16	rfp cfp		1	3			4
17	rfp cfp		3	1			4
18	rfp cfp		1	1			2
19	yfp cfp		1		1		2
20	yfp cfp		2		1		3
21	rfp yfp		1		1		2
22	rfp cfp		1		2		3
23	yfp cfp			1	1		2
24	rfp cfp			1	1		2
25	rfp yfp		4	2	2		8
26	yfp cfp		3	2			5
27	rfp cfp		4	2			6
28	rfp yfp		2	6			8
29	yfp cfp			3	3		6
30	yfp cfp		3				3
31	rfp cfp		4				4
32	yfp cfp		3				3
33	yfp cfp		3				3
34	rfp cfp				8		8
35	cfp				4		4
36	yfp cfp				4		4

FIGURE S3: Related to Figure 3. Clonal observations upon lineage tracing of premigratory and migratory NC cells.

Lists of the 2-8 cells clones observed in the *Wnt1-CreER^{T}* and *Sox10-CreER^{T2}* embryos both at low (S3A, S3B) and high (S3C, S3D) recombination densities. For each clone the following information is provided: category of statistical evidence for multipotency, derivatives where the clone was observed, number and color of the cells comprising the clone. The clones observed in the *Wnt1-CreER^{T}* line were obtained analyzing 7 *Wnt1-CreER$^{T\ low}$* embryos (14 DRG-units, 4 litters, S3A) and 18 *Wnt1-CreER$^{T\ high}$* embryos (36 DRG-units, 7 litters, S3C). The clones observed in the *Sox10-CreER^{T2}* line were obtained analyzing 4 *Sox10-CreER$^{T2\ low}$* embryos (9 DRG-units, 2 litters, S3B) and 10 *Sox10-CreER$^{T2\ high}$* embryos (22 DRG-units, 5 litters, S3D).

Figure S4 related to Figure 3

strong evidence for multipotency
substantial evidence for multipotency
weak evidence for multipotency
no evidence for multipotency

A Wnt1-CreER^{T}

Clone ID	Color	dNT	DRG	SG	VR	DLP	Tot
1	rfp cfp	3	14	10	2	2	31
2	rfp cfp	4	6	7	13	1	31
3	rfp yfp	9	1	4	2	1	17
4	rfp cfp	2	4	1		1	8
5	rfp yfp	3	55		3	3	64
6	rfp cfp	1		2		1	4
7	rfp cfp	1			1	1	3
8	yfp cfp	1	6	19	10		36
9	rfp yfp	1	7				8
10	rfp yfp	13			1		14
11	rfp yfp	1			1		2
12	rfp yfp	1			1		2
13	rfp yfp		7	5		5	17
14	rfp cfp		1		3	1	5
15	rfp cfp			1	1	2	4
16	rfp cfp		1	2	3		6
17	rfp cfp		11	1	1		13
18	yfp cfp		15	3	1		19
19	yfp cfp		3	6	6		15
20	rfp yfp		10	10	10		30
21	rfp cfp		2	1	2		5
22	rfp cfp		1	1	1		3
23	rfp cfp		4	2	1		7
24	rfp cfp		1	6			7
25	rfp yfp		2	1			3
26	rfp yfp		1	6			7
27	rfp cfp		10	1			11
28	rfp cfp		1	1			2
29	rfp yfp		1	3			4
30	rfp yfp			1	3		4
31	rfp yfp			1	3		4
32	rfp yfp			8	1		9
33	rfp cfp			1	2		3
34	rfp cfp			1	1		2
35	rfp cfp			1	1		2
36	rfp cfp	3	7	2			12
37	rfp cfp		7	21	6		34
38	rfp cfp		37	3	7		47
39	rfp cfp		8	7	16		31
40	rfp cfp		7	3	4		14
41	gfp		6	2			8
42	gfp		3	4			7
43	rfp cfp		2	5			7
44	rfp cfp		3		2		5
45	rfp cfp			3	2		5
46	rfp cfp			2	2		4
47	rfp yfp		9				9
48	rfp cfp		25				25
49	rfp cfp			4			4
50	rfp yfp			2			2
51	gfp			8			8
52	rfp yfp				6		6
53	rfp cfp				3		3
54	rfp cfp				5		5
55	rfp yfp				3		3

B Sox10-CreER^{T2}

Clone ID	Color	dNT	DRG	SG	VR	DLP	Tot
1	rfp yfp		16	3	1	2	22
2	rfp cfp		1	4	7	1	13
3	rfp yfp		4	1	4	2	11
4	rfp cfp		1	2	2	1	6
5	rfp yfp		2	1		1	4
6	rfp cfp				1	2	3
7	rfp cfp		3	1	1		5
8	rfp cfp		2	1	2		5
9	rfp yfp		1	1	1		3
10	rfp cfp		3	4	4		11
11	rfp yfp		5	11	1		17
12	rfp cfp		3	2	1		6
13	rfp yfp		1	4	1		6
14	rfp cfp		4	1	2		7
15	yfp cfp		5	1	2		8
16	rfp cfp		2	3	2		7
17	rfp yfp		3	1	1		5
18	rfp yfp		4	1	2		7
19	rfp yfp		1	1			2
20	yfp cfp		1	2			3
21	rfp cfp		1	1			2
22	yfp cfp		1	3			4
23	rfp cfp		3	1			4
24	yfp cfp		2		1		3
25	yfp cfp		1		1		2
26	rfp yfp		1		1		2
27	yfp cfp		1		2		3
28	rfp cfp			1	1		2
29	yfp cfp			1	1		2
30	rfp yfp		2	5	5		12
31	rfp yfp		4	2	2		8
32	rfp yfp		4	8	2		14
33	rfp yfp		2	7	15		24
34	rfp yfp		3	3	4		10
35	rfp yfp		7	2	3		12
36	rfp yfp		3	5	2		10
37	rfp yfp		2	6			8
38	yfp cfp		3	2			5
39	rfp cfp		4	2			6
40	rfp yfp		7		4		11
41	rfp yfp		10		9		19
42	yfp cfp			3	3		6
43	yfp cfp		3				3
44	yfp cfp		3				3
45	rfp cfp		4				4
46	yfp cfp		3				3
47	rfp cfp				8		8
48	yfp cfp				4		4

FIGURE S4: Related to Figure 3. Mathematical evaluation of NC cell fate determination for all the clones of the rare color category without size restriction.

List of the clonal frameworks for premigratory (S4A) and migratory (S4B) NC cells ordered by degree of evidence for multipotency. Both conditions of low and high recombination densities were pooled to compare the potentials of premigratory versus migratory NC cells. We listed and analyzed statistically all the clones with rare colors (rfp cfp, rfp yfp, yfp cfp, gfp) that were observed in 25 *Wnt1-CreER*^{T} embryos (50 DRG-units, 11 litters) and in 14 *Sox10-CreER*^{T2} embryos (31 DRG-units, 7 litters), respectively.

Table S1A related to Figure 1 and S1B related to Figure 2

A

	Wnt1-CreER$^{T\ low}$		Wnt1-CreER$^{T\ high}$		Sox10-CreER$^{T2\ low}$		Sox10-CreER$^{T2\ high}$	
	Average%	SEM (+/-)	Average%	SEM (+/-)	Aveage%	SEM (+/-)	Average%	SEM (+/-)
rfp 	48.69	5.47	41.48	2.91	72.69	7.91	43.50	2.64
yfp 	37.89	5.55	30.24	2.57	17.35	6.57	35.94	3.27
cfp 	12.06	2.87	22.62	2.52	9.18	3.28	14.58	1.69
rfp cfp 	0.95	0.37	3.25	0.85	0.33	0.33	1.43	0.29
rfp yfp 	0.28	0.13	1.93	0.90	0.07	0.07	3.53	0.45
yfp cfp 	0.12	0.10	0.30	0.18	n.o.	n.o.	1.01	0.21
gfp 	n.o.	n.o.	0.17	0.11	0.38	0.38	n.o.	n.o.
gfp rfp 	n.o.	n.o.	n.o.	n.o.	n.o.	n.o.	n.o.	n.o.
gfp yfp 	n.o.	n.o.	n.o.	n.o.	n.o.	n.o.	n.o.	n.o.
gfp cfp 	n.o.	n.o.	n.o.	n.o.	n.o.	n.o.	n.o.	n.o.

B

	Wnt1-CreER$^{T\ low}$		Wnt1Cre-ER$^{T\ high}$		Sox10-CreER$^{T2\ low}$		Sox10-CreER$^{T2\ high}$	
	Average%	SEM (+/-)	Average%	SEM (+/-)	Aveage%	SEM (+/-)	Average%	SEM (+/-)
dNT	14.02	2.11	7.64	1.28	n.o.	n.o.	n.o.	n.o.
DRG	40.91	3.62	49.58	1.87	38.70	4.77	50.55	1.30
SG	18.88	2.78	18.01	1.26	29.66	6.91	24.13	1.80
VR	16.63	3.10	20.88	1.53	20.44	4.00	24.48	1.74
DLP	9.55	1.83	3.88	0.86	11.19	3.90	0.84	0.40

TABLE S1 (A): Related to Figure 1. Frequency of color representations in NC cells traced by *R26R-Confetti*.

Frequency of the different color combinations represented in the Figure 1L and 1M for *Wnt1-CreER^{T}* and *Sox10-CreER^{T2}* embryos analyzed at low and high recombination densities. To calculate the color densities for the *Wnt1-CreER^{T}* line we analyzed 7 embryos (14 DRG-units, 4 litters) and 18 embryos (36 DRG-units, 7 litters) at low and at high recombination densities respectively. To measure the color frequencies for the *Sox10-CreER^{T2}* line we analyzed 4 embryos (9 DRG-units, 2 litters) and 10 embryos (22 DRG-units, 5 litters) at low and high recombination densities respectively. n.o. indicates not observed situations.

TABLE S1 (B): Related to Figure 2. Derivative representations upon *R26R-Confetti*-mediated NC cell tracing.

Percentage of recombined cells per NC derivatives for each of the four experimental setups. To calculate the percentage of recombined cells per derivative in the *Wnt1-CreER^{T}* line we analyzed 7 embryos (14 DRG-units, 4 litters) and 18 embryos (36 DRG-units, 7 litters) at low and at high recombination densities, respectively. For the *Sox10-CreER^{T2}* line we analyzed 4 embryos (9 DRG-units, 2 litters) and 10 embryos (22 DRG-units, 5 litters) at low and high recombination densities, respectively. n.o. indicates not observed situations.

Table S2A related to Figure 3, S3 and S2B related to Figure 4, S4

A

Clonal density for 2-8 cells cohorts

	Nr of clones	Nr of units	Nr of embryos	Nr of litters	Clones per unit
Wnt1-CreER$^{T\ low}$	14	14	7	4	1.0 ± 0.3
Wnt1-CreER$^{T\ high}$	29	36	18	7	0.8 ± 0.1
Sox10-CreER$^{T2\ low}$	11	9	4	2	2.2 ± 0.2
Sox10-CreER$^{T2\ high}$	36	22	10	5	1.6 ± 0.2

Clonal distribution per DRG-unit

Nr of clones per unit	0	%	1	%	2	%	3	%	>3	%	Total of units
Wnt1-CreER$^{T\ low}$	4	28.6	8	57.1	0	0	2	14.3	0	0	14
Wnt1-CreER$^{T\ high}$	16	44.4	11	30.6	9	25.0	0	0	0	0	36
Sox10-CreER$^{T2\ low}$	1	11.1	5	55.6	3	33.3	0	0	0	0	9
Sox10-CreER$^{T2\ high}$	2	9.1	8	36.4	8	36.4	4	18.1	0	0	22

B

Clonal density for cohorts of cells belonging to the rare color category

	Nr of clones	Nr of units	Nr of embryos	Nr of litters	Clones per unit
Wnt1-CreER$^{T\ low}$	11	14	7	4	1.7 ± 0.3
Wnt1-CreER$^{T\ high}$	64	77	36	14	0.8 ± 0.1
Sox10-CreER$^{T2\ low}$	1	9	4	2	0.1 ± 0.1
Sox10-CreER$^{T2\ high}$	63	45	18	9	1.4 ± 0.2

Clonal distribution per DRG-unit

Nr of clones per unit	0	%	1	%	2	%	3	%	>3	%	Total of units
Wnt1-CreER$^{T\ low}$	7	50.0	5	35.7	0	0	2	14.3	0	0	14
Wnt1-CreER$^{T\ high}$	32	41.5	31	40.3	9	11.7	5	6.5	0	0	77
Sox10-CreER$^{T2\ low}$	8	88.9	1	11.1	0	0	0	0	0	0	9
Sox10-CreER$^{T2\ high}$	12	26.7	13	28.9	10	22.2	10	22.2	0	0	45

TABLE S2 (A): Related to Figure 3 and S3. Clonal density analysis for cohorts of 2-8 cells.

The total number of clones, of DRG-units, of embryos, and of litters analyzed for each of the four experimental setups, *Wnt1-CreER^{T}* and *Sox10-CreER^{T2}* line both at low and at high recombination densities, are listed. The data refer to Figures 3 and S3. The average of clones per unit is provided ± SEM. To indicate the observed clonal distribution per DRG-unit, we listed the absolute numbers and the respective percentages of numbers of clones per DRG-unit.

TABLE S2 (B): Related to Figure 4 and S4. Clonal density analysis for cohorts of cells belonging to the rare color category (rfp cfp, rfp yfp, yfp cfp, gfp).

List of the total number of clones, of DRG-units, of embryos, and of litters analyzed for both *Wnt1-CreER^{T}* and *Sox10-CreER^{T2}* line at low and high recombination densities. The data refer to Figures 4 and S4. The average of clones per unit is provided ± SEM. The clonal distribution per DRG-unit is given by the absolute numbers and the respective percentages of numbers of clones observed per DRG-unit.

MOVIE S1: Related to Figure S2. 3D reconstruction of a DRG-unit.

Imaging of a Z stack of 316.7μm illustrates a space larger than the usual DRG-unit (an embryonic trunk segment with the width of a single DRG) used for the statistical analysis. 3D reconstruction of the left DRG of an E10.5 *Wnt1-CreER*$^{T\ high}$ embryo stained for neurofilament shows an example for the color combination rfp yfp and illustrates how seldom the mixed color combinations were observed: only two rfp yfp cells in the DRG.

MOVIE S2: Related to Figure S2. 3D reconstruction of part of the SG chain.

Imaging of a Z stack of 316.7μm shows part of the SG chain stained for neurofilament. In the whole stack we could observe only two cells with the fluorescent protein combination rfp yfp.

SUPPLEMENTAL EXPERIMENTAL PROCEDURES

Embryos numbers

Embryos numbers used in Figure 1

To calculate the color densities for the *Wnt1-CreER^{T}* line we analyzed 7 embryos (14 DRG-unit, 4 litters) and 18 embryos (36 DRG-unit, 7 litters) at low and at high recombination densities, respectively. To measure the color frequencies for the *Sox10-CreER^{T2}* line we analyzed 4 embryos (9 DRG-units, 2 litters) and 10 embryos (22 DRG-units, 5 litters) at low and high recombination densities, respectively.

Embryos numbers used in Figure 2

To calculate the percentage of recombined cells per derivative in the *Wnt1-CreER^{T}* line we analyzed 7 embryos (14 DRG-units, 4 litters) and 18 embryos (36 DRG-units, 7 litters) at low and high recombination densities, respectively. For the *Sox10-CreER^{T2}* line we analyzed 4 embryos (9 DRG-units, 2 litters) and 10 embryos (22 DRG-units, 5 litters), respectively.

Embryos numbers used in Figure 3

The clones observed in the *Wnt1-CreER^{T}* line were obtained analyzing 7 *Wnt1-CreER$^{T\ low}$* embryos (14 DRG-units, 4 litters) and 18 *Wnt1-CreER$^{T\ high}$* embryos (36 DRG-units, 7 litters). The clones observed in the *Sox10-CreER^{T2}* line were obtained analyzing 4 *Sox10-CreER$^{T2\ low}$* embryos (9 DRG-units, 2 litters) and 10 *Sox10-CreER$^{T2\ high}$* embryos (22 DRG-units, 5 litters).

Embryos numbers used in Figure 4

The clones of the *Wnt1-CreER^{T}* line were obtained by analyzing 18 *Wnt1-CreER$^{T\ high}$* embryos (41 DRG-units, 7 litters). The clones of the *Sox10-CreER^{T2}* line were obtained by analyzing 8 *Sox10-CreER$^{T2\ high}$* embryos (23 DRG-units, 4 litters).

Immunofluorescence, whole mount staining and SeeDB clearing

For immunohistochemistry, 10μm-thick cryosections were processed as previously described (John et al., 2011). Primary antibody was used as follows: mouse anti-NF160 (1:300; Sigma, N-5264), rabbit anti-Sox10 (1:250; Abcam, ab27655), mouse anti-Brn3a (1:100; Millipore, MAB1585), mouse anti-tyrosine hydroxylase (1:200; Sigma, T1299). As a secondary antibody the DyLight 649 Donkey anti-mouse IgG (H+L) (1:300; Jackson, 715-495-150), DyLight 649 Goat anti-rabbit (1:300; Jackson, 111-495-003), Alexa Fluor 488 Goat anti-mouse (1:300; Invitrogen, A-11029). *lacZ* reporter gene expression was detected as previously described (Hari et al., 2012). For 3D imaging the whole mount staining with anti-NF160 (1:250; Sigma, N-5264) and the SeeDB clearing protocol were applied as previously described (Ke et al., 2013).

Statistical analysis

Assumptions of the statistical model

The statistical analysis is based on the following assumptions:

1. Within each mouse line and recombination density, each embryo is independent
2. Within each embryo, each DRG-unit is independent
3. The development and migration is color-independent
4. Each mother cell leads to at least two cells
5. There is at most one mother cell per color and corresponding derivative(s)

These are typical assumptions and essentially imply: By 1 and 2, the individual sections from all embryos (within a particular mouse line and recombination) can be taken as replicates. The available data does not show any indication against these

assumptions. By 3, we can – by appropriately taking into account the relative color frequencies – use each color individually. At our current state of knowledge there is no competition between the individual colored cells. Assumption 4 implies that no mother cell gets lost or dies and that there is at least one replication. Assumption 5 is justified as we restrict the analysis to at most eight cells per color (for larger cell numbers see below).

In the following we describe in some detail how the probabilities of observing a particular configuration of cell counts (Figure 3, all the cohorts of 2-8 cells) in the five derivatives (dNT, DRG, SG, VR, DLP, Table S1B) for each color (Table S1A) under the respective framework (predetermination or multipotency) was calculated. The different colors appear with different relative expression frequencies, denoted by r_{color}. Similarly, the derivative sizes vary and the relative derivative sizes are denoted by d_{deriv}. These two quantities are unknown and we estimated their values from frequency tables (Figures 1L, 1M, 2G, and Table S1A, B). We assumed that each embryo and DRG-unit are independent from one another, and that embryonic development and cell migration are color-independent as well and thus the product $r_{\text{color}}\, d_{deriv}$ is the probability of observing the particular color in the particular derivative. We represented each configuration of cell counts as a quintuple (corresponding to the five derivatives) with binary entries, which equaled one if cells were observed in the corresponding derivative and zero otherwise. We denoted such a binary "observed" value with $o_{color.deriv}$ for any of the colors and five derivatives.

To calculate the probability of observing a particular configuration, we considered cases of mother cell configurations that lead to the corresponding configuration. Not all mother cell configurations develop with equal probability into the particular configuration and hence this probability has to be taken into account (this approach

is formally termed the of law of total probability). In the case of predetermination, the mother cell configuration is identical to the derivative configuration and thus, one only needs to calculate the probability of observing an identical mother cell configuration. This probability consists of the product of the probabilities of having a colored cell in the derivative whenever we observed one and of one minus that probability whenever we did not observe one:

$$P(\text{ configuration }) = P(\text{ mother cell configuration })$$

$$= \prod_{deriv} (r_{color} d_{deriv})^{o_{color.deriv}} (1-r_{color} d_{deriv})^{(1-o_{color.deriv})},$$

where r_{color}, d_{deriv} and $o_{color.deriv}$ are as above.

In the case of multipotent cells, it has to be taken into account that the clones migrate to the derivatives with probabilities according to the estimated derivative size (Figure 2G and Table S1B). The probability to observe a mother cell with a specific color is proportional to the relative expression frequency of that color (Figures 1L and 1M, Table S1A). Hence,

$$P(\text{ configuration }) = P(\text{ observing mother cell }) P(\text{ migration to derivatives })$$

$$= r_{color} \prod_{deriv} d_{deriv}^{o_{color.deriv}} (1-d_{deriv})^{(1-o_{color.deriv})}$$

where r_{color}, d_{deriv} and $o_{color.deriv}$ are as above.

The precise stochastic assumptions of the model, a sensitivity analysis of the involved parameters and further technical insights are given below.

Sensitivity Analysis

The cutoffs to classify the deviance (twice the negative log of the likelihood ratio) are -2log(.1), -2log(.01), -2log(.001) resulting in the (approximate) bins (-∞, 4.6), (4.6, 9.2), (9.2, 13.8) and (13.8, ∞) for “no”, “weak”, “substantial” and “strong” evidence. Choosing slightly different cutoffs does not change the result. In many cases, the weak and substantial bins are empty. Note that a zero deviance is equivalent to

equal probabilities of both frameworks and thus a “no”-evidence case does not imply that a predetermined case was more likely.

Figure 3D summarizes and compares the likelihoods when the minimum/maximum clone sizes are varied according to the pairs 4-8, 1-16, 2-16, 2-8, 2-6. The results do virtually not depend on these sizes.

We have also perturbed the values of the relative color frequencies (r_{color}) and relative derivative size (d_{deriv}) by multiplying them by a random number between 1/3 and 3 (uniformly distributed) followed by a rescaling. The analysis has been carried out as described above and the differences with respect to the classification for the evidence of multipotency has been recorded. Figure 3E shows the results for 100 of such simulations. Each of the 16 barplots shows the proportion of the 100 cases that changed, white indicates no change, redish to red cases that are added and greenish to green cases that are lost. For the low recombination rates, the results are virtually the same (white dominates the barplots). For the high recombination rates moderate changes occur. For example, for the results of the analysis of the *Sox10-CreER*$^{T2\ \text{high}}$ embryos, 1/36 of the cases are classified as substantial evidence (clone ID 25, Figure S3D). In one third of the perturbed cases this proportion has not changed. In one fifth of the cases there is no case marked as substantial evidence and in 33% (10%, 2%) there are 2/36 (3/36 and 4/36) cases marked as substantial evidence, respectively.

Additional Comments

The presented methodology is “frequency based”. Naturally, a Bayesian framework would be possible. In such a framework, priori information about our beliefs in multipotency needs to be specified and then enters the calculations. A fully Bayesian specification would imply that all other parameters (relative color frequencies, relative derivative sizes, etc.) would need to be considered as random and would be

equipped with a priori distribution. We do not have any priori knowledge about these parameters and “uniform”/uninformative priors would be the only possible choice. Such a uniform priori would essentially lead to the same result as a frequency setting.

The calculation of the configuration probabilities for both the predetermined and multipotency cases can be unified through the use of the law of total probability. More precisely, these probabilities can be expressed as follows.

$P(\text{ configuration }) = \Sigma_k P(\text{ configuration } | \text{ mother cell configuration } k) P(\text{ mother cell configuration } k)$

In the case of predetermination, the mother cell configuration is identical to the derivative configuration; hence the conditional probabilities are equal to one in the case the derivative configuration is equal to the mother cell configuration and zero otherwise. A particular mother cell configuration is characterized by having or not having the colored cell in a particular derivative. Therefore,

$P(\text{ configuration }) = P(\text{ same mother cell configuration })$

$$= \Pi_{deriv} (r_{color} d_{deriv})^{ocolor.deriv} (1-r_{color} d_{deriv})^{(1-ocolor.deriv)},$$

where r_{color}, d_{deriv} and $o_{color.deriv}$ are as in the main text.

In the case of multi-fated cells, the mother cell configuration is derivative independent and consists of a particularly colored clone (all other colored cells lead to zero conditional probability). It has to be taken into account that the clones migrate to the derivatives with probabilities according to the estimated derivative size. This migration is color independent. Hence

$P(\text{ configuration }) = P(\text{ configuration } | \text{ mother cell with appropriate color }) P(\text{ mother cell with appropriate color }) = \Pi_{deriv} d_{deriv}^{ocolor.deriv} (1-d_{deriv})^{(1-ocolor.deriv)} r_{color}$

where r_{color}, d_{deriv} and $o_{color.deriv}$ are as above.

Assumption 5 excludes the possibility of several mother cells in the case of multipotency as well. These cases are (statistically) very rare compared to one single mother cell. Among these few cases, some would be manifested as predetermination

and could not be used to discern the frameworks. All others would slightly increase the probability of observing multipotency and thus shift the deviances in direction towards “strong evidence”. Hence, we can safely ignore these rare cases.

SUPPLEMENTAL REFERENCES

John, N., Cinelli, P., Wegner, M., and Sommer, L. (2011). Transforming growth factor β-mediated Sox10 suppression controls mesenchymal progenitor generation in neural crest stem cells. Stem Cells *29*, 689–699.

Ke, M.-T., Fujimoto, S., and Imai, T. (2013). SeeDB: a simple and morphology-preserving optical clearing agent for neuronal circuit reconstruction. Nat Neurosci *16*, 1154–1161.

Short summary of 100 words

The neural crest (NC) is an embryonic cell population with one of the broadest developmental potentials. However, it is debated whether individual NC cells *in vivo* are multipotent or whether the NC is comprised of heterogeneous lineage-restricted progenitors. Here, we resolve this controversy by performing *in vivo* fate mapping of trunk NC cells at premigratory and migratory stages using the *R26R-Confetti* model. By combining quantitative clonal analyses with definitive markers of differentiation, we demonstrate that the majority of both premigratory and migrating NC cells in the mouse are multipotent *in vivo*.

Supplemental Movies & Spreadsheets

Click here to download Supplemental Movies & Spreadsheets: Movie S1.avi

Supplemental Movies & Spreadsheets

Click here to download Supplemental Movies & Spreadsheets: Movie S2.avi